Bioconjugate Chemistry

Article

pubs.acs.org/bc

Bile Acid Conjugated DNA Chimera that Conditionally Inhibits Carbonic Anhydrase-II in the Presence of MicroRNA-21

Xiaozhu Chu,[†] Cooper H. Battle,[†] Nan Zhang,[†] Gyan H. Aryal,[†] Madhusoodanan Mottamal,[‡] and Janarthanan Jayawickramarajah*[,†]

[†]Department of Chemistry, Tulane University, 2015 Percival Stern Hall, New Orleans, Louisiana 70118, United States

[‡]RCMI Cancer Research Center, Xavier University of Louisiana, New Orleans, Louisiana 70125, United States

Supporting Information

ABSTRACT: In order to tackle the issue of systemic toxicity in chemotherapy, there is a need to develop novel mechanisms for the activation of protein inhibitors using biomarkers overexpressed in cancer cells. Many current strategies focus on using cancer associated enzymes as a triggering agent for prodrugs. Herein, we detail an alternative approach that harnesses a microRNA (miR-21) that is overexpressed in cancers as the trigger that activates an inhibitor of human carbonic anhydrase-II (hCA-II). Specifically, we have developed a DNA-small molecule chimera (DC) composed of an hCA-II binding lithocholic acid amide (LAA) headgroup that can transition from a rigid duplex state (that does not bind appreciably to hCA) to a single-stranded conformation via a miR-21 trigger. The activated single-stranded DC can project the LAA headgroup into the hCA-II active site and is a robust hCA-II inhibitor (K_i of 3.12 μM). This work may spur research into developing new classes of cancer selective protein inhibitors.

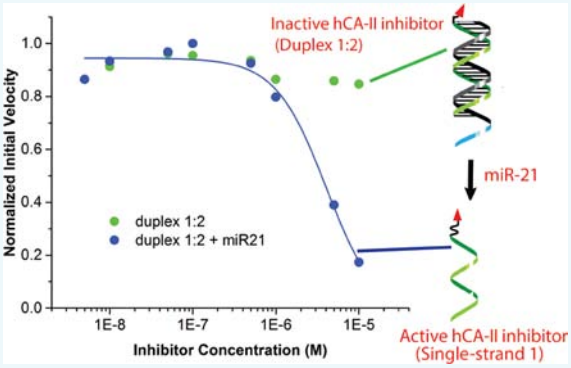

INTRODUCTION

Conventional cancer therapeutics often exhibit decreased drug efficacy and significant systemic toxicity due to nonspecific biodistribution. To achieve site selective drug action there has been much exploration of nanocarriers and cytotoxic small molecules conjugated to targeting ligands.[1−9] A complementary strategy is to use prodrugs that are conditionally activated by molecules localized in cancer tissue.[10−14] Harnessing such endogenous stimuli is an appealing route, inter alia, because—unlike external inputs—there is no requirement for specialized and expensive equipment. The major approach utilized for molecular activation of prodrugs via endogenous inputs is to exploit the covalent transformations afforded by tumor-associated enzymes.[13−18] Although a salient strategy, for each disease-associated enzyme that is harnessed one needs to laboriously design and optimize the corresponding prodrug structure. Additionally, disease-associated enzymes often have isoforms present in healthy tissue and generating isoform selective agents remains a formidable challenge.[19−21]

In contrast to enzymes, oligonucleotides (ONs) are informational and many cancer-associated ONs with unique sequences have been identified. Thus, the development of pharmacophores that are activated by cancer-associated ONs is an attractive route for prodrug generation. In this regard, microRNAs (miRs) are especially important biomarkers because a single miR can regulate the translation of multiple unique mRNAs and therefore has a significant role in disease progression.[22−24] In particular, miR-21 is a critical miR that promotes tumor development by inhibiting the translation of key tumor suppressor genes and hence is overexpressed in various cancers including breast, colon, prostate, and lung.[25] In addition, miR-21 overexpression is correlated with cancer aggressiveness/stage,[26,27] and drug resistance.[28]

A number of elegant strategies for ON templated triggering of inactive molecules and protein inhibitors have been reported.[29−49] These systems have largely centered on DNA templation that leads to an intramolecular covalent reaction.[29−35] However, an issue with this strategy is the need for specialized bio-orthogonal reactions (to minimize side reactions with reactive biomolecules). In addition, once activated such systems cannot be further controlled (i.e., they lack reversibility). A complementary approach is to use the molecular recognition and subsequent conformational changes of ONs that are tethered to protein recognition elements (such as nucleic acids, small molecules, and peptides)[36−41] to develop allosteric protein binders.[42−49] To the best of our knowledge, there is no report of using such ON hybrids to inhibit a protein in conditional response to a cancer-associated miR.[50] With this article, we disclose a novel DNA-small molecule chimera (DC **1**) system that can inhibit human carbonic anhydrase-II (hCA-II) upon activation by miR-21 (see Figure 1).

Received: April 23, 2015
Revised: July 4, 2015
Published: July 20, 2015

DOI: 10.1021/acs.bioconjchem.5b00231
Bioconjugate Chem. 2015, 26, 1606−1612

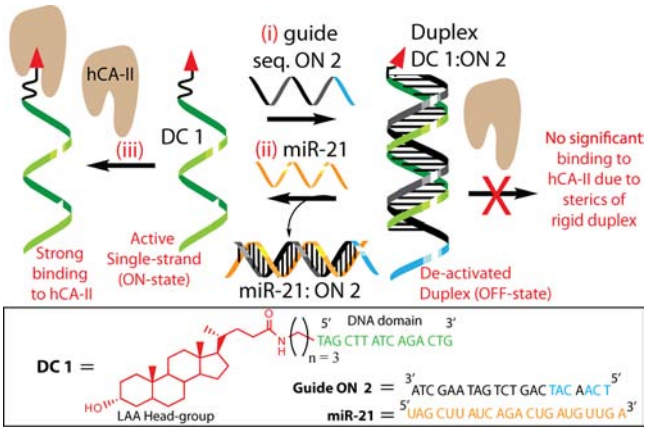

Figure 1. Illustration depicting miR-21 induced activation of a DC based hCA-II inhibitor. (i) A toe-hold containing duplex is formed between DC **1** and an LNA guide sequence **2**. This duplex sterically hinders the lithocholic acid amide headgroup (red arrowhead) from binding to the active site of hCA-II. (ii) In response to miR-21, which is fully complementary to ON **2**, the more stable miR-21:ON **2** duplex is formed, thereby releasing the single-stranded DC **1**. (iii) Activated and flexible single-stranded DC **1** is a strong binder of hCA-II. Inset: Summary of the key ON sequences used in this study. Note: The sequence in blue for ON **2** depicts the LNA residues.

RESULTS AND DISCUSSION

HCA-II was chosen as the target protein to be inhibited because it is a cytosolic member of a family of metalloenzymes (hCAs) that catalyze the conversion of CO_2 to bicarbonate ion and a proton. While bicarbonate is a substrate for critical biological pathways (including gluconeogenesis and nucleotide synthesis), the production of protons can lead to pH changes. Both of these hCA based effects are thought to be important in providing tumors with a growth advantage over normal tissue.[51,52] Thus, hCA inhibitors are being actively pursued.[53] Although we are targeting hCA-II in this study, it is important to note that the potential cancer selectivity of this system lies in its ability to use miR-21 as the overexpressed cancer biomarker to specifically activate the inhibitor in tumor tissues.

The design and function of DC **1** is shown in Figure 1. DC **1** contains a bile acid headgroup (specifically, a lithocholic acid amide, LAA) since bile acids are known to interact with hCA-II.[54,55] The LAA headgroup was attached to the core ON domain via a short C3 linker. This linker length was specifically utilized since in the single-stranded state DC **1** can project the LAA moiety into the conical and deep (15 Å) active site of hCA-II.[56,57] However, the function of DC **1** can be turned OFF by hybridization with a complementary guide sequence (ON **2**) because the rigid duplex in conjunction with the short linker prevents the optimal positioning of the LAA headgroup into the active site.[58] Furthermore, ON **2** contains a non-base-paired toehold and is fully complementary to miR-21. Hence, in the presence of miR-21 the DC **1**:ON **2** duplex is expected to disassemble resulting in the formation of the ON **2**:miR-21 duplex and single-stranded DC **1** (which is able to effectively inhibit hCA-II). For the design of guide ON **2**, six locked nucleic acid (LNA)[59] residues were incorporated into the toehold region since LNA based ONs have superior hybridization capacity with RNA.[60]

UV−visible spectroscopy and polyacrylamide gel electrophoresis (PAGE) were employed to probe the self-assembly characteristics of DC **1**. In particular, since hydrophobic

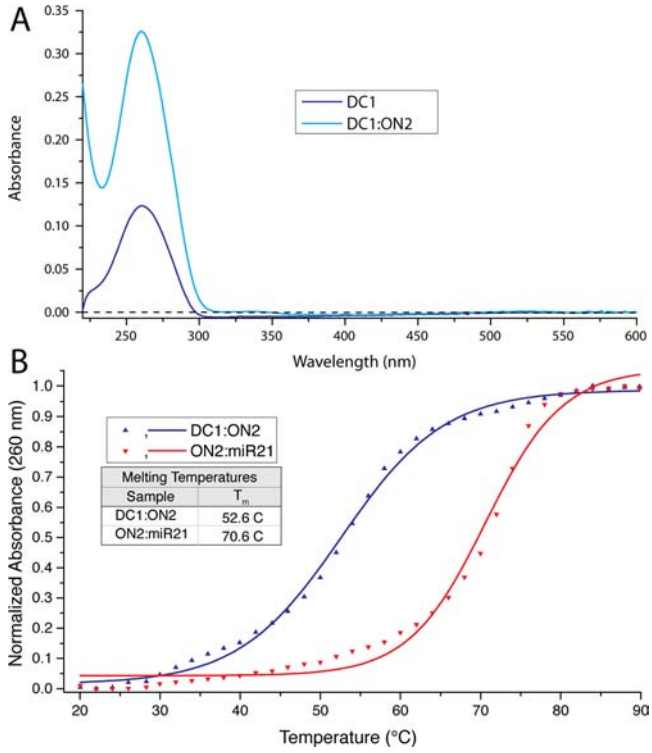

Figure 2. (A) UV−vis spectra of DC**1** and DC**1**:ON**2** duplex at 20 °C. (B) Thermal denaturation curves of DC**1**:ON**2** and ON**2**:miR-21 duplexes. All spectra were collected in a 100 μM Tris-NaCl buffer at 7.1 pH with 1 μM ON strand concentrations.

molecule-conjugated ONs[61−65] can potentially form micelles, we investigated whether a low concentration (1 μM) of DC **1** shows such aggregation behavior. As can be seen from inspection of Figure 2A, both DC **1** and the DC **1**:ON **2** duplex (at 1 μM concentrations) exhibit characteristic absorption profiles centered around 260 nm, and show near-baseline absorption at long wavelengths—indicating a lack of aggregate-based scattering. Further, when DC **1** was analyzed by nondenaturing PAGE (Figure 3A, Lane 1) only a single, fast-moving band, corresponding to a single strand, was observed. There was no indication of any slow-migrating higher-order species. Taken together, these findings are consistent with no significant self-aggregation induced by the hydrophobic LAA headgroup in the 1 μM regime.

Next, UV−vis derived thermal denaturation studies were performed on both the DC **1**:ON **2** and the miR-21:ON **2** duplexes (Figure 2B). These experiments clearly suggested that the latter duplex is significantly more thermally stable (T_m greater by 18 °C) and thus exposure to miR-21 should drive the disassembly of the DC **1**:ON **2** duplex. In order to probe this structural conversion process PAGE was employed (Figure 3A). Here it is evident that upon addition of 1 equiv. of miR-21, the preformed DC **1**:ON **2** duplex (Lane 4) disassembles leading to the miR-21:ON **2** duplex and single-stranded DC **1** (Lane 6). Fluorescence spectroscopy was also conducted to verify the miR-21 induced structure switching (Figure 3B). Here, an internal deoxycytidine residue (C7 from the 3′ end) of DC **1** was replaced with the fluorescent cytidine analogue pyrrolo-2′-deoxycytidine (pdC). The pdC containing strand DC **1F** should show strong fluorescence in a single-stranded, non-base-paired, conformation. However, when hybridized with guide ON **2** the fluorescence is expected to be quenched.[66]

DOI: 10.1021/acs.bioconjchem.5b00231
Bioconjugate Chem. 2015, 26, 1606−1612

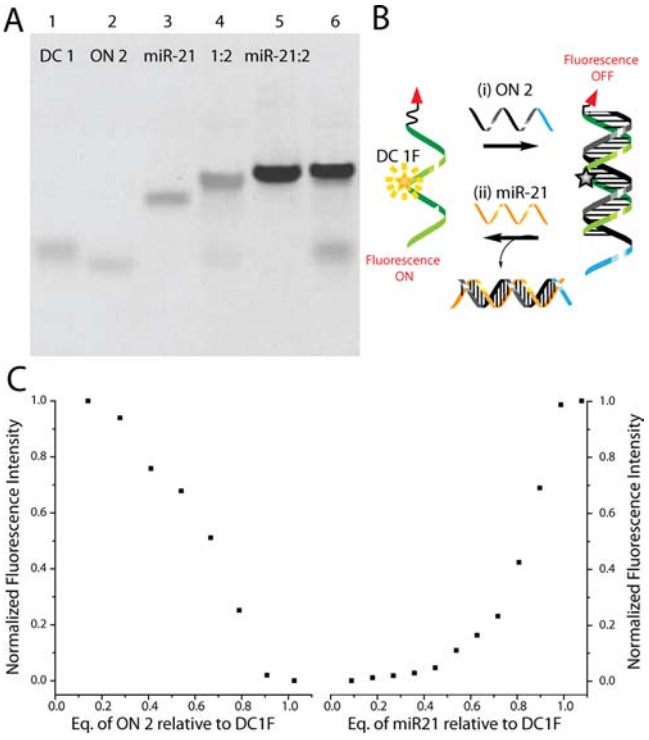

Figure 3. (A) PAGE illustrating miR21-induced structure switching of DC **1**. Lanes 1−5: ON single strand or duplex controls. Lane 1, DC **1**; Lane 2, ON **2**; Lane 3, miR-21; Lane 4, duplex **1:2**; Lane 5, duplex miR-21:**2**. Lane 6: The structure switching experiment: DC **1** + ON **2** (incubated for 30 min) followed by addition of miR-21 (incubated for 30 min). (B) Schematic of the pdC based fluorescence assay. (i) Fluorescence is quenched when pdC is base-paired with guanine in the DC **1F:2** duplex, and then (ii) recovered upon addition of miR-21 when single-stranded **1F** is released via the formation of the more stable miR-21:**2** duplex. (C) Results of the fluorescence assay. Left: Fluorescence quenching of **1F** upon hybridization with ON **2**. Right: Fluorescence recovery of **1F** induced by miR-21. Excitation λ = 345 nm and emission λ = 450 nm; these experiments were conducted in 0.2 M NaCl, 0.1 M Tris, pH = 7.4, buffer.

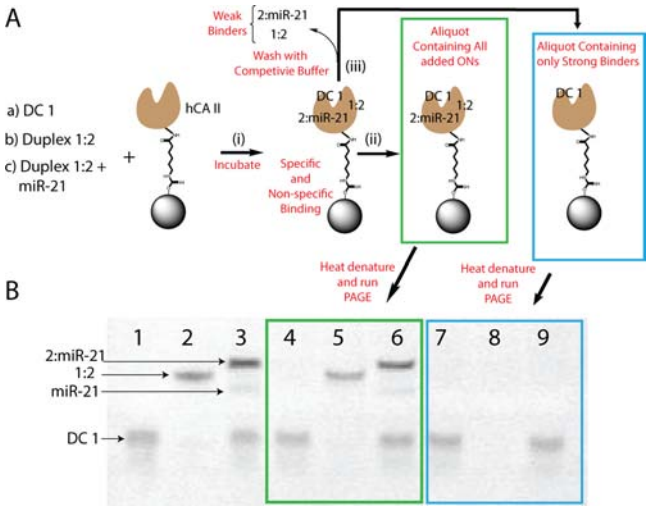

Figure 4. (A) hCA-II binding assay. (i) The three tested ON species were incubated with hCA-II immobilized on a solid support. (ii) An aliquot of the unwashed sample (containing all nonspecifically/specifically bound ONs) was denatured with heat and run on the gel. (iii) An aliquot of sample washed with a competitive buffer (to select for the strong binding ON species) was denatured with heat and run on the gel. (B) PAGE results of the hCA-II solid-phase binding assay. Lanes 1−3: ON controls. Lane 1, DC **1**; Lane 2, ONs **1**/**2**; Lane 3, ONs **1**/**2**/miR-21. Lanes 4−6: Unwashed aliquots. Lane 4, DC **1**; Lane 5, ONs **1**/**2**; Lane 6, ONs **1**/**2**/miR-21. Lanes 7−9: Aliquots washed with competitive buffer. Lane 7, DC **1**; Lane 8, ONs **1**/**2**; Lane 9, ONs **1**/**2**/miR-21.

Moreover, addition of miR-21 should lead to recovery of fluorescence as the single-stranded DC **1F** is regenerated. The fluorescence experiment (Figure 3C) commenced with the titration of ON **2** into a solution of 1 μM of DC **1F**. After the addition of 1 equiv. of ON **2**, the fluorescence signal reached a plateau. Subsequently, miR-21 was titrated into the equimolar solution of DC **1F** and ON **2**. Importantly, when 1 equiv. of miR-21 relative to DC **1F** was added, the fluorescence was fully recovered indicating stoichiometric responsiveness. These fluorescence studies verified the miR-21 induced structure switching mechanism observed by PAGE.

Having demonstrated that miR-21 can induce the structure-switching of duplex **1:2** into single-stranded DC **1**, we next investigated whether the single-stranded and duplex states of DC **1** showed differential binding to hCA-II via a solid-phase binding assay (see Figures 4A and 6). Briefly, hCA-II was immobilized on a solid *N*-hydroxysuccinimidyl-sepharose bead support and was exposed to the following three ON species (in 10 mM Tris, 0.1 M NaCl, pH 7.4 buffer) to test for their binding abilities to hCA-II: (a) single-stranded DC **1**, (b) duplex **1:2**, and (c) a solution containing duplex **1:2** that was incubated with 1 equiv. of miR-21. After incubation of these ON samples with hCA-II (at 4 °C for 5 h), each sample was separated into two equal portions and the incubation buffer removed via centrifugal filters. The first portion of resin stayed unwashed (thus all the added ONs are expected to be present). On the other hand, to the second aliquot was introduced competitive washing solutions (see Experimental Section for details) so that only the strongly interacting species would remain bound to hCA-II. Subsequently, both aliquots of resins were resuspended in water, overlaid with 50 μL of mineral oil, and incubated at 90 °C for 30 min to denature hCA-II and release the bound ON species. After denaturation, the aqueous layers were analyzed by PAGE.

As shown in Figure 4B, for the unwashed aliquots (Lane 4−6), all the introduced ON species are observed. Not surprisingly, after competitive washing to remove the weak binders, the **2:**miR-21 duplex that lacks the hCA-II binding headgroup is not present on the gel, as it was washed away (compare the missing slow migrating band on Lane 9 that is observed on Lane 6). Moreover, the DC **1:2** duplex also does not appear on the gel (compare the missing band on Lane 8 that is present on Lane 5) as it does not bind appreciably with hCA-II—since the double-stranded structure inhibits the LAA headgroup from binding effectively with hCA-II. Indeed the only ON species that survived the washing step was the single-stranded DC **1** either when introduced by itself (Lane 7) or when released from duplex **1:2** by miR-21 (Lane 9). These results indicate that the miR-21 triggered formation of DC **1** leads to substantial binding of hCA-II, while duplex **1:2** does not interact significantly with the protein.

We next probed, via a solution-phase colorimetric assay, whether the esterase activity of hCA-II is differentially affected by the duplex and single-stranded states of DC **1**. Figure 5 shows the normalized initial reaction velocity versus inhibitor concentration. As expected, single-stranded DC **1** inhibited the

DOI: 10.1021/acs.bioconjchem.5b00231
Bioconjugate Chem. 2015, 26, 1606−1612

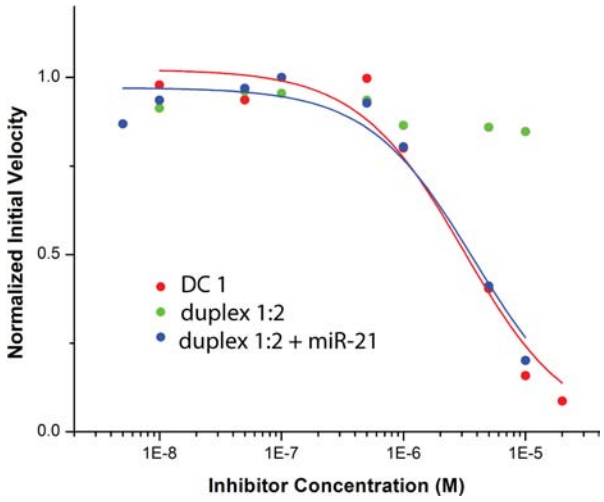

Figure 5. hCA-II inhibition profiles. The concentrations of hCA-II and *p*-NPA were 124 nM and 1 mM, respectively.

esterase activity of hCA-II with a K_i of 2.56 μM. In marked contrast, no significant inhibitory activity was observed for duplex **1:2** under the same experimental conditions. Importantly, in the presence of miR-21, the sample containing inactive duplex **1:2** exhibits hCA-II inhibition that is similar to that of DC **1** by itself (K_i value of 3.12 μM). Taken together, these results clearly demonstrate that the OFF state of DC **1** (i.e., duplex **1:2**) is activated by miR-21, thereby leading to a state that inhibits the hCA-II esterase function.

CONCLUSIONS

We have developed a single-stranded LAA modified DC-based inhibitor against hCA-II that can be deactivated using a guide LNA containing strand **2**. This OFF state is postulated to be a result of the short linker and the steric hindrance introduced by the rigid duplex structure. Strikingly, in the presence of miR-21, the guide strand forms a more stable duplex with miR-21, thereby triggering the activation of the single-stranded inhibitor. This is the first report of using a conformationally restrained protein inhibitor that is noncovalently triggered by a microRNA. The strategy described above is expected to be broadly applicable to prodrug development since the sequence of the core ON domain of the DC can be modified to target other cancer-associated miRs and the synthetic ligand can be interchanged to bind to alternative active sites of target proteins. In addition, because simple sequestration of miR-21, via duplex formation, can silence its oncogenic activity,[68,69] this strategy has the potential to be synergistic. We are currently investigating DC activity in vivo using cancer cell lines overexpressing miR-21.

EXPERIMENTAL PROCEDURES

Unless specially noted all chemicals were obtained from Sigma-Aldrich. All core oligonucleotide (ON) sequences, except guide ON sequence **2**, were synthesized by the Keck Foundation Biotechnology Research Laboratory at Yale University using automated solid-phase synthesis. LNA containing ON **2** was synthesized by Exiqon. The nonstandard, modified phosphoramidites (pyrrolo dC, 5′-amino Modifier C3 TFA, 5′-amino Modifier C6 PDA, and 5′-amino Modifier C12) were purchased from Glen Research. All ONs were desalted with Sephadex resin Microspin G-25 columns (GE Healthcare), and purified via a Varian Prostar reverse-phase HPLC system. The purified product was analyzed by Matrix Assisted Laser Desorption Ionization-Time of Flight (MALDI-TOF) mass spectrometry using a Bruker Daltonics Autoflex III in reflector negative mode. All MALDI-TOF samples were prepared by mixing 3-hydroxypicolinic acid (HPA, 50 mg/mL in 1:1 water/acetonitrile), ammonium citrate (50 mg/mL in water), and ON at a 9:1:1 ratio. The concentrations of the ON stock solutions were determined by the use of UV spectrophotometry based on the molar extinction coefficient at 260 nm as determined by the nearest-neighbor method. Fluorescence spectroscopy was conducted using a Varian Cary Eclipse Fluorescence spectrophotometer. The hCA-II inhibition assay was performed using a SpectraMax 190 microplate reader. Detailed syntheses of head groups and ON-conjugates can be found in the SI.

Thermal Denaturation. Thermal denaturation was followed by UV−vis absorption changes at 260 nm. Melting temperatures (T_m) were determined by fitting the collected data to a Boltzmann sigmoidal function in OriginPro 9.1.

Gel Electrophoresis. The 14% polyacrylamide TBE gel was prepared by mixing 3.5 mL of 40% acrylamide solution, 1 mL of 1 × TBE buffer, and 5.5 mL of water, followed by the addition of 50 μL of 10% ammonium persulfate (APS) and 10 μL of *N,N,N′,N′*-tetramethylethylenediamine (TEMED). The gel-forming solution was stirred for a couple of seconds, and then poured between the glass plates and a comb was inserted to form the gel.

For single-stranded ONs (DC **1**, ON **2**, and miR-21) the samples were prepared in 10 μL of water with an ON concentration of 2 μM. The duplex ON samples (DC **1**:ON **2** and ON **2**:miR-21) were prepared by incubating the two ONs (2 μM for each) in 10 μL of water at RT for 30 min. The structure switching sample was prepared by incubating DC **1** and ON **2** (2 μM for each) in 10 μL of water at RT for 30 min, then adding 1 equiv. of miR-21 and incubating the three ONs at RT, for another 30 min. The samples then were applied onto the gel and subjected to electrophoresis at a constant voltage of 120 V for 1 h with 1 × TBE running buffer. After electrophoresis, the gel was visualized by ethidium bromide staining.

HCA-II Immobilization. One milliliter of *N*-hydroxysuccinimidyl-Sepharose 4 Fast Flow slurry was placed in an Amicon centrifugal filter (cutoff: 10K) and spun to remove isopropanol, followed by washing with (a) 3 × 2 mL of cold 1 mM HCl and (b) 2 mL of cold water. hCA-II was dissolved in 500 μL of 1 × PBS buffer pH 7.1 at a concentration of 16 μM (hCA-II concentration was determined by UV−vis spectrometry). The hCA-II solution was incubated with the beads at 4 °C overnight. After removing the coupling solution, the beads were capped using 600 μL of 50 mM Tris-HCl buffer pH 8.3 for 3 h. After extensive washing with 3 × 2 mL of 10 mM Tris-HCl, 1 M NaCl buffer, pH 7.4, the beads were stored in 650 μL of 10 mM Tris-HCl, 0.1 M NaCl buffer, pH 7.4, at 4 °C.

Solid-Phase HCA-II Binding Assays. Three species were tested for their binding abilities to hCA-II: (a) single-stranded inhibitor DC **1** (2 μL of 0.1 mM in water), (b) DC **1**:ON **2** duplex (formed by incubating 2 μL of 0.1 mM DC **1** with 1 equiv. of ON **2** in water at RT for 30 min, total volume was 4 μL), and (c) DC **1**:ON **2**:miR21 (formed by incubating 2 μL of 0.1 mM DC **1** with 1 equiv. of ON **2** at RT for 30 min, followed by the addition of 1 equiv. of miR-21, and incubation for another 30 min; total volume was 6 μL). Each of these

DOI: 10.1021/acs.bioconjchem.5b00231
Bioconjugate Chem. 2015, 26, 1606−1612

samples (i.e., a, b, and c) was added to an Eppendorf tube containing 80 μL of a bead suspension conjugated with hCA-II, followed by addition of 10 mM Tris, pH 7.4, 0.1 M NaCl buffer to reach a final volume of 200 μL.

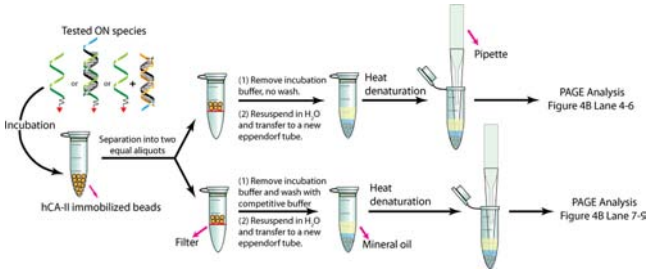

Figure 6. Illustration of the procedure for the solid-phase hCA-II binding assay.

The Eppendorf tube was agitated at 4 °C for 5 h, then the mixture was separated into two equal aliquots (100 μL of each) and both were transferred to centrifugal filters (cutoff: 30K) to remove the incubation buffers (Figure 6). For comparison purposes, the first aliquot of dry resin stayed unwashed while the second aliquot was washed with a competitive series of solutions: (1) 400 μL of 10 mM Tris, pH 7.4, 0.5 M NaCl, (2) 2 × 400 μL of 10 mM Tris, pH 7.4, 0.1 M NaCl, and (3) 400 μL of water. Both aliquots of dry resin were then resuspended in 30 μL of water and overlaid with 50 μL of mineral oil, followed by incubation at 90 °C for 30 min to denature hCA-II. After denaturation, the bottom aqueous solution was pipetted out and allowed to cool down to RT over a period of 30 min, then analyzed by PAGE as described above.

Solution-Phase hCAII Inhibition Studies. The hCA-II inhibition assay was conducted by dissolving hCA-II in 50 mM Tris-sulfate pH 8.5, and incubating in a 96-well plate with a dilution series of inhibitors for 30 min at R.T. Subsequently, the reaction was initiated by adding substrate, *p*-nitrophenyl actetate (*p*-NPA). The UV−vis absorption change at 405 nm, corresponding to the production of *p*-nitrophenolate was recorded.

Normalization of the initial reaction velocity was performed by assigning a maximum value of 1 to the initial reaction velocity obtained from an hCA-II esterase activity assay in the absence of any inhibitor for each series of experiments. Specific initial reaction velocities in the presence of inhibitors in these studies were converted to proportions of this value (ranging from 0 to 1).

The normalized initial reaction velocity (V_0) was plotted against the corresponding inhibitor concentration (I), and the K_i (the dissociation constant of the enzyme−inhibitor complex) value was obtained by fitting, via nonlinear regression, to eq 1[67] below using Origin software. S is the final concentration of the substrate *p*-NPA, which is 1 mM.

$$v = \frac{V_{max}[S]}{[S] + K_m\left(1 + \frac{[I]}{K_i}\right)} \quad (1)$$

The Michaelis−Menten constant K_m and the V_{max} values (V_{max} is a maximal limit of the rate of an enzyme-catalyzed reaction and K_m is defined by the substrate concentration that gives a reaction rate equal to one-half the V_{max}) were first obtained for *p*-NPA hydrolysis catalyzed by hCA-II in the absence of inhibitors (See SI-5).

■ ASSOCIATED CONTENT

Supporting Information

The Supporting Information is available free of charge on the ACS Publications website at DOI: 10.1021/acs.bioconjchem.5b00231.

Detailed synthesis and characterization of DCs, modeling, effect of linker length on the inhibitory ability of the DCs, and the effect of LNA bases on mismatch discrimination (PDF)

■ AUTHOR INFORMATION

Corresponding Author

*E-mail: jananj@tulane.edu.

Notes

The authors declare no competing financial interest.

■ ACKNOWLEDGMENTS

We gratefully acknowledge the NIH for supporting both the experimental (grant R01GM097571 to J.J.) and modeling portions of this work (2G12MD007595). C.H.B thanks the NSF for a graduate fellowship.

■ REFERENCES

(1) Lehner, R., Wang, X., Marsch, S., and Hunziker, P. (2013) Intelligent nanomaterials for medicine: carrier platforms and targeting strategies in the context of clinical application. *Nanomedicine 9*, 742−57.

(2) Zhong, Y., Meng, F., Deng, C., and Zhong, Z. (2014) Ligand-Directed Active Tumor-Targeting Polymeric Nanoparticles for Cancer Chemotherapy. *Biomacromolecules 15*, 1955−1969.

(3) Allen, T. M. (2002) Ligand-targeted therapeutics in anticancer therapy. *Nat. Rev. Cancer 2*, 750−63.

(4) Liu, Q., Jin, C., Wang, Y., Fang, X., Zhang, X., Chen, Z., and Tan, W. (2014) Aptamer-conjugated nanomaterials for specific cancer cell recognition and targeted cancer therapy. *NPG Asia Mater. 6*, e95.

(5) Chari, R. V. J. (2008) Targeted Cancer Therapy: Conferring Specificity to Cytotoxic Drugs. *Acc. Chem. Res. 41*, 98−107.

(6) Song, L., Ho, V. H. B., Chen, C., Yang, Z., Liu, D., Chen, R., and Zhou, D. (2013) Efficient, pH-Triggered Drug Delivery Using a pH-Responsive DNA-Conjugated Gold Nanoparticle. *Adv. Healthcare Mater. 2*, 275−280.

(7) Blum, A. P., Kammeyer, J. K., Rush, A. M., Callmann, C. E., Hahn, M. E., and Gianneschi, N. C. (2015) Stimuli-Responsive Nanomaterials for Biomedical Applications. *J. Am. Chem. Soc. 137*, 2140−2154.

(8) Jensen, S. A., Day, E. S., Ko, C. H., Hurley, L. A., Luciano, J. P., Kouri, F. M., Merkel, T. J., Luthi, A. J., Patel, P. C., Cutler, J. I., et al. (2013) Spherical nucleic acid nanoparticle conjugates as an RNAi-based therapy for glioblastoma. *Sci. Transl. Med. 5*, 209ra152/1−209ra152/12 12.

(9) Ryu, J.-H., Chacko, R. T., Jiwpanich, S., Bickerton, S., Babu, R. P., and Thayumanavan, S. (2010) Self-Cross-Linked Polymer Nanogels: A Versatile Nanoscopic Drug Delivery Platform. *J. Am. Chem. Soc. 3*, 2−10.

(10) Singh, Y., Palombo, M., and Sinko, P. J. (2008) Recent trends in targeted anticancer prodrug and conjugate design. *Curr. Med. Chem. 15*, 1802−1826.

(11) Rautio, J., Kumpulainen, H., Heimbach, T., Oliyai, R., Oh, D., Järvinen, T., and Savolainen, J. (2008) Prodrugs: design and clinical applications. *Nat. Rev. Drug Discovery 7*, 255−70.

(12) Zawilska, J. B., Wojcieszak, J., and Olejniczak, A. B. (2013) Prodrugs: a challenge for the drug development. *Pharmacol. Rep. 65*, 1−14.

DOI: 10.1021/acs.bioconjchem.5b00231
Bioconjugate Chem. 2015, 26, 1606−1612

(13) Cui, J., and Li, S. (2014) Inhibitors and Prodrugs Targeting CYP1: A Novel Approach in Cancer Prevention and Therapy. *Curr. Med. Chem. 21*, 519−552.
(14) Tietze, L. F., and Schmuck, K. (2011) Prodrugs for targeted tumor therapies: recent developments in ADEPT, GDEPT and PMT. *Curr. Pharm. Des. 17*, 3527−3547.
(15) Rooseboom, M., Commandeur, J. N. M., and Vermeulen, N. P. E. (2004) Enzyme-catalyzed activation of anticancer prodrugs. *Pharmacol. Rev. 56*, 53−102.
(16) Schüller, J., Cassidy, J., Dumont, E., Roos, B., Durston, S., Banken, L., Utoh, M., Mori, K., Weidekamm, E., and Reigner, B. (2000) Preferential activation of capecitabine in tumor following oral administration to colorectal cancer patients. *Cancer Chemother. Pharmacol. 45*, 291−7.
(17) Tanaka, A., Fukuoka, Y., Morimoto, Y., Honjo, T., Koda, D., Goto, M., and Maruyama, T. (2015) Cancer-cell death induced by the intracellular self-assembly of an enzyme-responsive supramolecular gelator. *J. Am. Chem. Soc. 137*, 770−775.
(18) Chien, M.-P., Carlini, A. S., Hu, D., Barback, C. V., Rush, A. M., Hall, D. J., Orr, G., and Gianneschi, N. C. (2013) Enzyme-Directed Assembly of Nanoparticles in Tumors Monitored by in Vivo Whole Animal Imaging and ex Vivo Super-Resolution Fluorescence Imaging. *J. Am. Chem. Soc. 135*, 18710−18713.
(19) Alterio, V., Di Fiore, A., D'Ambrosio, K., Supuran, C. T., and De Simone, G. (2012) Multiple binding modes of inhibitors to carbonic anhydrases: how to design specific drugs targeting 15 different isoforms? *Chem. Rev. 112*, 4421−68.
(20) Agrawal, A., Romero-Perez, D., Jacobsen, J. a, Villarreal, F. J., and Cohen, S. M. (2008) Zinc-binding groups modulate selective inhibition of MMPs. *ChemMedChem 3*, 812−20.
(21) Balasubramanian, S., Verner, E., and Buggy, J. J. (2009) Isoform-specific histone deacetylase inhibitors: the next step? *Cancer Lett. 280*, 211−21.
(22) Ambros, V. (2004) The functions of animal microRNAs. *Nature 431*, 350−355.
(23) Bartel, D. P. (2004) MicroRNAs: Genomics, biogenesis, mechanism, and function. *Cell 116*, 281−297.
(24) Hammond, S. M. (2006) MicroRNA therapeutics: a new niche for antisense nucleic acids. *Trends Mol. Med. 12*, 99−101.
(25) Krichevsky, A. M., and Gabriely, G. (2009) MiR-21: a small multi-faceted RNA. *J. Cell. Mol. Med. 13*, 39−53.
(26) Calin, G. a, and Croce, C. M. (2006) MicroRNA signatures in human cancers. *Nat. Rev. Cancer 6*, 857−66.
(27) Esquela-Kerscher, A., and Slack, F. J. (2006) Oncomirs - microRNAs with a role in cancer. *Nat. Rev. Cancer 6*, 259−69.
(28) Allen, K. E., and Weiss, G. J. (2010) Resistance may not be futile: microRNA biomarkers for chemoresistance and potential therapeutics. *Mol. Cancer Ther. 9*, 3126−36.
(29) Okamoto, A., Tanabe, K., Inasaki, T., and Saito, I. (2003) Phototriggered drug release from functionalized oligonucleotides by a molecular beacon strategy. *Angew. Chem., Int. Ed. 42*, 2502−4.
(30) Janssen, B. M. G., Lempens, E. H. M., Olijve, L. L. C., Voets, I. K., van Dongen, J. L. J., de Greef, T. F. A., and Merkx, M. (2013) Reversible blocking of antibodies using bivalent peptide−DNA conjugates allows protease-activatable targeting. *Chem. Sci. 4*, 1442.
(31) Shibata, A., Ito, Y., and Abe, H. (2013) RNA-templated molecule release induced protein expression in bacterial cells. *Chem. Commun. 49*, 270−2.
(32) Ma, Z., and Taylor, J.-S. (2000) Nucleic acid-triggered catalytic drug release. *Proc. Natl. Acad. Sci. U. S. A. 97*, 11159−11163.
(33) Rothlingshofer, M., Gorska, K., and Winssinger, N. (2011) Nucleic Acid-Templated Energy Transfer Leading to a Photorelease Reaction and its Application to a System Displaying a Nonlinear Response. *J. Am. Chem. Soc. 133*, 18110−18113.
(34) Erben, A., Grossmann, T. N., and Seitz, O. (2011) DNA-triggered synthesis and bioactivity of proapoptotic peptides. *Angew. Chem., Int. Ed. 50*, 2828−32.
(35) Li, X., and Liu, D. R. (2004) DNA-templated organic synthesis: nature's strategy for controlling chemical reactivity applied to synthetic molecules. *Angew. Chem., Int. Ed. 43*, 4848−70.
(36) Kim, Y., Cao, Z., and Tan, W. (2008) Molecular assembly for high-performance bivalent nucleic acid inhibitor. *Proc. Natl. Acad. Sci. U. S. A. 105*, 5664−9.
(37) Melkko, S., Zhang, Y., Dumelin, C. E., Scheuermann, J., and Neri, D. (2007) Isolation of high-affinity trypsin inhibitors from a DNA-encoded chemical library. *Angew. Chem., Int. Ed. 46*, 4671−4674.
(38) Eberhard, H., Diezmann, F., and Seitz, O. (2011) DNA as a molecular ruler: interrogation of a tandem SH2 domain with self-assembled, bivalent DNA-peptide complexes. *Angew. Chem., Int. Ed. 50*, 4146−50.
(39) Tagore, D. M., Sprinz, K. I., Fletcher, S., Jayawickramarajah, J., and Hamilton, A. D. (2007) Protein recognition and denaturation by self-assembling fragments on a DNA quadruplex scaffold. *Angew. Chem., Int. Ed. 46*, 223−5.
(40) Simon, P., Dueymes, C., Fontecave, M., and Décout, J.-L. (2005) DNA detection through signal amplification by using NADH: flavin oxidoreductase and oligonucleotide-flavin conjugates as cofactors. *Angew. Chem., Int. Ed. 44*, 2764−7.
(41) Diezmann, F., and Seitz, O. (2011) DNA-guided display of proteins and protein ligands for the interrogation of biology. *Chem. Soc. Rev. 40*, 5789−801.
(42) Röglin, L., Ahmadian, M. R., and Seitz, O. (2007) DNA-controlled reversible switching of peptide conformation and bioactivity. *Angew. Chem., Int. Ed. 46*, 2704−7.
(43) Portela, C., Albericio, F., Eritja, R., Castedo, L., and Mascareñas, J. L. (2007) ds-Oligonucleotide-Peptide Conjugates Featuring Peptides from the Leucine-Zipper Region of Fos as Switchable Receptors for the Oncoprotein Jun. *ChemBioChem 8*, 1110−1114.
(44) Dittmer, W. U., Reuter, A., and Simmel, F. C. (2004) A DNA-based machine that can cyclically bind and release thrombin. *Angew. Chem., Int. Ed. 43*, 3550−3.
(45) Saghatelian, A., Guckian, K. M., Thayer, D. A., and Ghadiri, M. R. (2003) DNA Detection and Signal Amplification via an Engineered Allosteric Enzyme. *J. Am. Chem. Soc. 125*, 344−345.
(46) Harris, D. C., Chu, X., and Jayawickramarajah, J. (2008) DNA-small molecule chimera with responsive protein-binding ability. *J. Am. Chem. Soc. 130*, 14950−14951.
(47) Harris, D. C., Saks, B. R., and Jayawickramarajah, J. (2011) Protein-binding molecular switches via host-guest stabilized DNA hairpins. *J. Am. Chem. Soc. 133*, 7676−9.
(48) Battle, C., Chu, X., and Jayawickramarajah, J. (2013) Oligonucleotide-Based Systems for Input-Controlled and Non-Covalently Regulated Protein-Binding. *Supramol. Chem. 25*, 37−41.
(49) Zhou, C., Yang, Z., and Liu, D. (2012) Reversible Regulation of Protein Binding Affinity by a DNA Machine. *J. Am. Chem. Soc. 134*, 1416−1418.
(50) Recently an elegant report was published wherein miR-21 is used as a trigger to release doxorubicin from mesoporous silica coated nanoparticles Zhang, P., Cheng, F., Zhou, R., and Cao, J. (2014) DNA-Hybrid-Gated Multifunctional Mesoporous Silica Nanocarriers for Dual-Targeted and MicroRNA-Responsive Controlled Drug Delivery. *Angew. Chem. 53*, 2371−5 In contrast, the current study investigates an allosteric prodrug activation mechanism instead of a nanocarrier based drug release strategy..
(51) Thiry, A., Dogné, J.-M., Masereel, B., and Supuran, C. T. (2006) Targeting tumor-associated carbonic anhydrase IX in cancer therapy. *Trends Pharmacol. Sci. 27*, 566−73.
(52) Pastorekova, S., Zatovicova, M., and Pastorek, J. (2008) Cancer-associated carbonic anhydrases and their inhibition. *Curr. Pharm. Des. 14*, 685−698.
(53) Supuran, C. T., Scozzafava, A., and Casini, A. (2003) Carbonic anhydrase inhibitors. *Med. Res. Rev. 23*, 146−189.
(54) Boone, C. D., Tu, C., and McKenna, R. (2014) Structural elucidation of the hormonal inhibition mechanism of the bile acid cholate on human carbonic anhydrase II. *Acta Crystallogr., Sect. D: Biol. Crystallogr. 70*, 1758−63.

DOI: 10.1021/acs.bioconjchem.5b00231
Bioconjugate Chem. 2015, 26, 1606−1612

(55) Milov, D. E., Jou, W. S., Shireman, R. B., and Chun, P. W. (1992) The effect of bile salts on carbonic anhydrase. *Hepatology 15*, 288−296.
(56) Eriksson, A. E., Jones, T. A., and Liljas, A. (1988) Refined structure of human carbonic anhydrase II at 2.0 Å resolution. *Proteins: Struct., Funct., Genet. 4*, 274−282.
(57) Avvaru, B. S., Kim, C. U., Sippel, K. H., Gruner, S. M., Agbandje-McKenna, M., Silverman, D. N., and McKenna, R. (2010) A short, strong hydrogen bond in the active site of human carbonic anhydrase II. *Biochemistry 49*, 249−51.
(58) For the effect of linker length on DC binding to hCA-II, see SI-2 (for hCA-II inhibition assays) and SI-3 (for modeling studies).
(59) Singh, S. K., Nielsen, P., Koshkin, A. A., and Wengel, J. (1998) LNA (locked nucleic acids): synthesis and high-affinity nucleic acid recognition. *Chem. Commun.*, 455−456.
(60) Thomsen, R., Nielsen, P. S., and Jensen, T. H. (2005) Dramatically improved RNA in situ hybridization signals using LNA-modified probes. *RNA 11*, 1745−1748.
(61) Gryaznov, S. M., and Lloyd, D. H. (1993) Modulation of oligonucleotide duplex and triplex stability via hydrophobic interactions. *Nucleic Acids Res. 21*, 5909−5915.
(62) Bleczinski, C. F., and Richert, C. (1999) Steroid−DNA Interactions Increasing Stability, Sequence-Selectivity, DNA/RNA Discrimination, and Hypochromicity of Oligonucleotide Duplexes. *J. Am. Chem. Soc. 121*, 10889−10894.
(63) Rosemeyer, H. (2005) Nucleolipids: Natural Occurrence, Synthesis, Molecular Recognition, and Supramolecular Assemblies as Potential Precursors of Life and Bioorganic Materials. *Chem. Biodiversity 2*, 977−1063.
(64) Laing, B. M., Barrow-Laing, L., Harrington, M., Long, E. C., and Bergstrom, D. E. (2010) Properties of Double-Stranded Oligonucleotides Modified with Lipophilic Substituents. *Bioconjugate Chem. 21*, 1537−1544.
(65) Serien, D., Grimm, C., Liebscher, J., Herrmann, A., and Arbuzova, A. (2014) DNA-controlled aggregation of virus like particles - mimicking a tetherin-like mechanism. *New J. Chem. 38*, 5181−5185.
(66) Zhang, X., and Wadkins, R. M. (2009) DNA hairpins containing the cytidine analog pyrrolo-dC: structural, thermodynamic, and spectroscopic studies. *Biophys. J. 96*, 1884−1891.
(67) Brandt, R. B., Laux, J. E., and Yates, S. W. (1987) Calculation of inhibitor Ki and inhibitor type from the concentration of inhibitor for 50% inhibition for Michaelis-Menten enzymes. *Biochem. Med. Metab. Biol. 37*, 344−9.
(68) Yang, M., and Mattes, J. (2008) Discovery, biology and therapeutic potential of RNA interference, microRNA and antagomirs. *Pharmacol. Ther. 117*, 94−104.
(69) Krützfeldt, J., Rajewsky, N., Braich, R., Rajeev, K. G., Tuschl, T., Manoharan, M., and Stoffel, M. (2005) Silencing of microRNAs in vivo with "antagomirs. *Nature 438*, 685−9.

DOI: 10.1021/acs.bioconjchem.5b00231
Bioconjugate Chem. 2015, 26, 1606−1612